Journal of Geochemical Exploration 230 (2021) 106848

Contents lists available at ScienceDirect

Journal of Geochemical Exploration

journal homepage: www.elsevier.com/locate/gexplo

Dissolution kinetics and solubilities of copper sulfides in cyanide and hydrogen peroxide leaching: Applications to increase selective extractions

Fernando Medina Ferrer [a,b,c,*], Bernhard Dold [d,e], Oscar Jerez [f]

[a] Advanced Mining Technology Center, College of Physical and Mathematical Sciences, University of Chile, Santiago, Chile
[b] Department of Geology, College of Physical and Mathematical Sciences, University of Chile, Santiago, Chile
[c] Department of Biochemistry and Molecular Biology, College of Chemical and Pharmaceutical Sciences, University of Chile, Santiago, Chile
[d] Sustainable Mining Research & Consultancy (SUMIRCO), San Pedro de la Paz (Biobio), Chile
[e] Pontifical Catholic University of Peru (PUCP), Lima, Peru
[f] Instituto de Geología Económica Aplicada, Universidad de Concepción, Concepción, Chile

ARTICLE INFO

Keywords:
Cyanidation
Leaching kinetics
Porphyry copper
Selective dissolution
Sequential extraction
Tailings

ABSTRACT

Accurate quantification of secondary and primary sulfide minerals is fundamental for resource evaluation, ore processing, and long-term sustainability of mining operations. In addition to visual mapping and automated mineral quantification, chemical analysis can also be harnessed to characterize the mineralogy of ore deposits. By evaluating the conditions in which certain minerals can be selectively dissolved from others, a chemical evaluation could provide geochemical speciation data of low-abundance minerals, such as copper/iron sulfides present in low-grade copper ores. The selective dissolution of copper sulfide minerals is, however, understudied. Here, we evaluate the use of potential selective dissolution conditions to differentiate supergene copper sulfides from hypogene copper sulfides. By characterizing the dissolution kinetics of chalcocite, covellite, bornite, enargite, chalcopyrite, and pyrite concentrates, we found that alkaline cyanidation (and not hydrogen peroxide or acid leaching in the presence of oxidizing agents) selectively dissolves supergene copper sulfides, which can be applied in a sequential extraction scheme to estimate the sulfide mineralogy of tailings samples. Cyanide completely dissolved chalcocite and covellite within 5–15 min, whereas dissolution in acid oxidative media only partially dissolved copper sulfides. Pyrite, chalcopyrite, enargite, and bornite under 0.5% KCN leaching (1 mg/mL) for 10 min showed approximately 1, 10, 30, and 40% of copper recovery, respectively. Cyanide leaching applied in sequential extractions of porphyry copper tailings samples from the Piuquenes impoundment, La Andina, Chile, improved the selective dissolution of secondary sulfides compared to a previously proposed hydrogen peroxide dissolution method, thus allowing their differentiation from primary sulfide minerals. The selective leaching of supergene sulfides by cyanidation provides a cheap and efficient method to estimate the copper sulfide mineralogy in copper ores, facilitating the sustainability and resource evaluation of mining operations.

1. Introduction

Mineral quantification of ore deposits is fundamental for resource estimation, definition of metallurgical extraction processes, and prediction of potential acid mine drainage (AMD) release from mine waste (e.g., Abrosimova et al., 2015; Fox et al., 2017; Gray and Van Rythoven, 2020; Velásquez et al., 2020). The complex mineral assemblage in ore bodies, however, greatly challenges large-scale mineralogical quantification efforts. In porphyry copper deposits, the sulfide mineralogy is composed of hypogene and supergene sulfides; the former represented by a variety of primary minerals, such as chalcopyrite and pyrite; the latter occurring as a replacement of primary sulfides throughout the supergene enrichment zone, usually in the form of secondary chalcocite-covellite group minerals (Lichtner and Biino, 1992; Ossandón et al., 2001; Dold, 2010). Hypogene and supergene copper sulfides not only differ in their relative metal quantity (which determines the ore grade), but they also define the appropriate extractive metallurgical approach (e.g., Scheffel et al., 2016; Barton et al., 2018; Bicak, 2019). In addition, different copper/iron sulfides vary greatly in their potential to generate AMD, thus controlling future mitigation strategies of the mine residues

* Corresponding author at: Department of Molecular and Cell Biology, University of California, Berkeley, CA, USA.
E-mail address: medinaferrer@berkeley.edu (F. Medina Ferrer).

https://doi.org/10.1016/j.gexplo.2021.106848
Received 23 June 2019; Received in revised form 14 June 2021; Accepted 30 June 2021
Available online 3 July 2021

(Carbone et al., 2013; Blowes et al., 2014; Elghali et al., 2018; Guseva et al., 2021). Therefore, differentiating between hypogene and supergene sulfide minerals in porphyry copper ores is crucial for resource estimation, downstream mineral processing and metallurgical extraction, as well as accurate assessment of potential environmental impacts. Our goal is to develop a cost-effective sulfide quantification alternative that would allow a reliable differentiation between hypogene and supergene copper sulfide minerals, applicable to sulfidic ore and tailings samples.

In transition zones, where hypogene minerals meet the supergene zone, several copper/iron sulfides co-occur at different proportions. The quantification of sulfide minerals in transition zones is, however, usually carried out by imprecise visual core mapping and/or optical point-counting analysis, which is costly and time-consuming when a large amount of samples are analyzed. In the last two decades, the development of automated quantitative mineralogy techniques has been important to improve the mineralogical characterization of ore deposits (Pooler and Dold, 2017; Guanira et al., 2020). However, automated mineralogy techniques fail to identify trace elements in the crystalline lattice, and thus a combination with wet chemical analysis (e.g., mineral digestion followed by AAS or ICP-MS) is often used to complement mineralogical characterizations. Cost-effective chemical analyses (such as cut-off estimates by total copper quantification) are therefore widely used. The utility of chemical analyses to provide mineralogical interpretations is, however, very limited, unless specific minerals can be selectively dissolved and the mineralogy further interpreted based on the dissolved elements. Incorporation of selective dissolution techniques to complement mineralogical quantifications has successfully been applied in the context of both partial and sequential extractions (e.g., Filipek and Theobald Jr, 1981; Dold and Fontboté, 2001, 2002; Dold and Weibel, 2013; Preece et al., 2018; Roebbert et al., 2018). However, the selective dissolution of copper sulfide minerals that commonly occur in porphyry copper deposits has been poorly studied. Consequently, the quantification of copper/iron sulfides (such as chalcopyrite, pyrite, bornite, chalcocite, and covellite) based on selective extraction methods has yet to be developed. Here, we explore some dissolution conditions that may allow for the differentiation of commonly occurring supergene sulfides from hypogene sulfides in a sequential extraction scheme.

Sequential extractions use different chemical digestion steps to progressively dissolve the same sample (Sahuquillo et al., 2003; Sutherland, 2010; Cuvier et al., 2021). If a leaching step selectively dissolves certain minerals, a mineralogical interpretation can then be made on the basis of dissolved elements in the leachate (e.g., Hall et al., 1996; Caraballo et al., 2013; Torres and Auleda, 2013; Khorasanipour, 2015; Consani et al., 2019). Despite the importance of copper sulfides in both metal availability and acid release, there is no standard procedure to selectively dissolve supergene from hypogene sulfides. Selective leaching of sulfide minerals was explored in the seven-step sequential extraction procedure proposed by Dold (2003a), in which a fifth leaching step using 35% hydrogen peroxide is used to dissolve supergene sulfides only, differentiating them from hypogene sulfides (Fig. 1; Table S1; Sondag, 1981; Hall et al., 1996; Dold and Fontboté, 2001, 2002; Dold, 2003a). The application of hydrogen peroxide leaching as part of the sequential extraction of diverse porphyry copper samples containing chalcopyrite as the main copper/iron-bearing sulfide suggests, however, that chalcopyrite may be highly susceptible to hydrogen peroxide leaching (Dold and Fontboté, 2001, 2002; Dold and Weibel, 2013; as well as unpublished data). Chalcopyrite dissolution by hydrogen peroxide treatment prevents the differentiation between secondary and primary sulfide minerals when using the sequential extraction approach proposed by Dold (2003a). It is essential, therefore, to characterize the dissolution of sulfide minerals by kinetic analyses (e.g., Dold, 2003b). In this study, the hydrogen peroxide dissolution step described by Dold (2003a) was assessed using chalcopyrite, pyrite, bornite, enargite, chalcocite, and covellite concentrates. To improve the selectivity of the technique, the dissolution kinetics of sulfide concentrates were evaluated under acid oxidative and alkaline cyanidation leaching conditions. An optimized method was obtained and used in porphyry copper tailings samples to test the selectivity of secondary sulfide dissolution in the context of a sequential extraction scheme.

2. Materials and methods

2.1. Mineral samples

Dissolution kinetic experiments were performed either using sulfide concentrates or tailings samples. The tailings samples were taken from different depths (1.0, 1.5, 2.0, 2.95, 4.0, 5.0, 7.0, and 9.0 m) of an oxidation profile of the Piuquenes tailings impoundment, La Andina porphyry copper deposit, Chile (Dold and Fontboté, 2001). The mineral concentrates included the supergene sulfides chalcocite (Cu_2S) and covellite (CuS), and the hypogene sulfides bornite (Cu_5FeS_4), enargite (Cu_3AsFe_4), chalcopyrite ($CuFeS_2$), and pyrite (FeS_2). Altogether, these minerals typically compose the main sulfide assemblage of porphyry copper ores (Dold and Fontboté, 2001; Ossandón et al., 2001). Covellite, bornite, and pyrite samples were hand-collected from natural specimens. Chalcocite, chalcopyrite, and enargite concentrates were enriched by froth flotation of porphyry copper-molybdenum deposits from Chile. Mineral samples were crushed and grounded with a ring mill. The portions bellow 38 μm were collected, washed with cold 1 M HCl for 15 min,

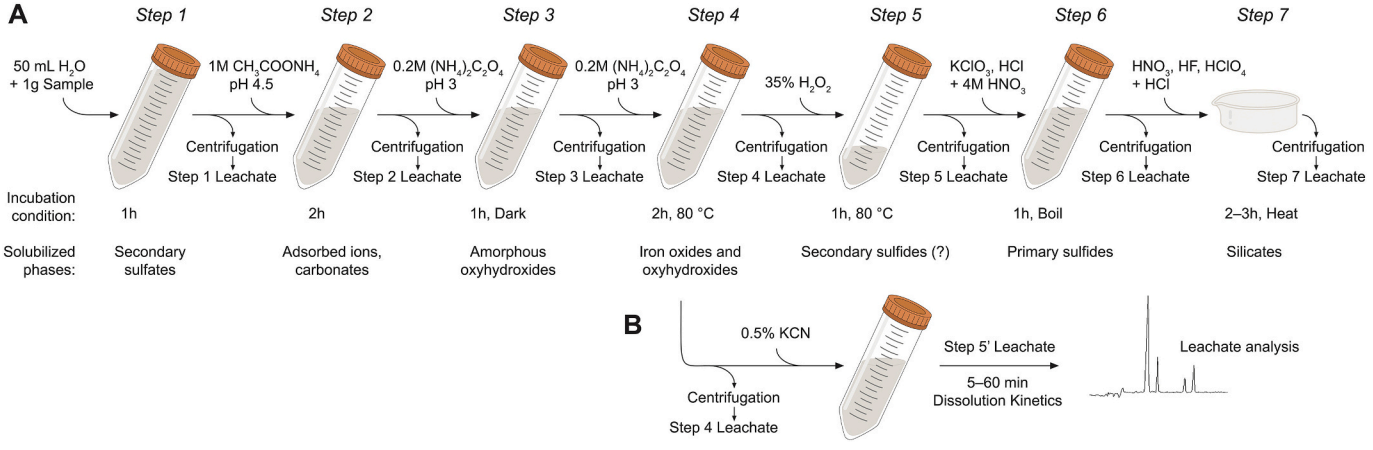

Fig. 1. Sequential extraction scheme. (A) Diagram of the seven-step sequential extraction procedure proposed by Dold (2003a). One gram of sample is progressively incubated with solutions that preferentially dissolve specific mineral phases. At each step, the leachate is recovered by centrifugation and the dissolved elements are quantified, whereas the solid residue is used for the subsequent leaching step. (B) A modification of the fifth step evaluated in this study.

vacuum filtered (0.45 μm), rinsed with distilled water, and dried at 150 °C. The cold acid wash was used to remove potential oxide coatings on the surface of the sulfides prior to the dissolution kinetic experiments.

Mineral identification and evaluation of impurities were determined by powder X-ray diffraction (XRD) using a Bruker D8 Advance X-ray diffractometer with CuKα radiation (λ = 1.5406 Å) at 40 kV and 20 mA. Scans were collected using a 0.02° 2θ step interval and 18.9–28.2 s counting time per step (Table S2).

2.2. Leaching experiments

Hydrogen peroxide leaching was applied as described in the fifth step of the sequential extraction procedure after Dold (2003a; Fig. 1; Table S1). Five milliliters of a 35% H_2O_2 solution (Thermo Fisher Scientific, Waltham, MA, USA) was added to 0.1 g of sulfide concentrate in a 50 mL centrifuge tube for three replicate samples. The tube was then incubated in a hot water bath (approximately 80 °C) agitated every 10 min for 1 h (Table S1). The supernatant was obtained by vacuum filtration (0.45 μm) and the sulfide residue was washed twice with 5 mL of distilled water. The water washes were mixed with the hydrogen peroxide extraction solution and adjusted to 25 mL before its analysis (Section 2.3).

A 500 mL three-neck flat-bottom flask was used for the dissolution kinetic experiments of the mineral concentrates. The reaction flask was equipped with a thermometer and a condenser. The third neck of the flask was closed with a ground-glass stopper and was used to take aliquots of 1 mL at time points of 5, 10, 15, 25, 40, 60, 90, and 120 min from a single dissolution experiment for each concentrate and condition tested. The flask was incubated in a 25 °C water bath, and the dissolution reaction was initiated by adding 200 mg of sulfide concentrate to 200 mL of the leaching solution (prepared with milli-Q water previously purged with N_2) while agitating with a magnetic stirrer at 750 rpm. After taking a sample at each time point, 1 mL of fresh solution was added back into the reaction flask to keep a constant solid-to-liquid ratio (1 mg/mL). The samples were immediately filtered with 0.2 μm syringe filters before their analysis for element quantification (Section 2.3).

Cyanidation kinetics of tailings samples were performed by end-over-end rocking of 50 mL centrifuge tubes containing 1*g* of sample and 25 mL of either 0.5% or 1.0% KCN solution. The leaching with 1.0% KCN corresponded to a partial extraction (e.g., no previous dissolution steps) for 1 h, whereas the incubation with 0.5% KCN was applied after the fourth step of the sequential extraction procedure described by Dold (2003a), where aliquots at 5, 10, 15, 25, 40, and 60 min were taken for analysis. The sequential extraction procedure (Fig. 1; Table S1) consisted of a first-step incubation with 50 mL of distilled water for 1 h, followed by a second leaching step with 20 mL of a solution 1 M ammonium acetate pH 4.5 for 2 h, a third incubation step for 1 h in the dark with 20 mL 0.2 M ammonium oxalate adjusted to pH 3.0 with 0.2 M oxalic acid, and a fourth step consisting of an 80 °C incubation for 2 h (with agitation every 10 min) using 20 mL 0.2 M ammonium oxalate adjusted to pH 3.0 with 0.2 M oxalic acid. All reagents used were from Sigma-Aldrich (St. Luis, MO, USA), unless otherwise indicated. After each sequential extraction step, the supernatant was obtained by centrifugation (6000 ×*g* for 5 min) of the 50 mL tube, and the residue was washed twice with 5 mL of distilled water. The fifth step of the sequential extraction corresponded either to a 35% hydrogen peroxide incubation (Dold, 2003a), or to a 0.5% KCN incubation. For the hydrogen peroxide step, the residue was incubated with 5 mL 35% H_2O_2 (Thermo Fisher Scientific) in a water bath at 80 °C for 1 h with agitation every 10 min. For the cyanide incubation, the residue of the fourth step [$(NH_4)_2C_2O_2$ pH 3.0 leach] was additionally washed with 1 mL 0.1 M KOH to neutralize acid traces (recommended to avoid the potential release of toxic HCN fumes) and then incubated for 1 h with 0.5% KCN at room temperature.

Total Cu and Fe in the sulfide concentrates were estimated by complete dissolution of the sample in acid oxidative medium (step 7 of the sequential extraction, Table S1; Dold, 2003a). Five milliliters HNO_3, 7.5 mL HF, and 2.5 mL $HClO_4$ were added to 200 mg of sulfide sample in a polytetrafluoroethylene evaporating dish and heated on a hotplate until complete evaporation of the solution (~2 h). Five milliliters of water and 2.5 mL HCl were added to dissolve the remaining salts under heating. The final solution was adjusted to 25 mL with distilled water. For metal quantification, two parts of the extract was neutralized with one part of 10 M KOH. The neutralized fraction was redissolved and diluted with 100 mM KCN, and the soluble metal-cyano complexes were quantified by capillary zone electrophoresis as described in the Section 2.3. The total copper or iron content obtained from each sample was used to calculate the dissolution percentage in the leaching experiments.

2.3. Element quantification

Samples taken from the dissolution kinetic experiments with acid solutions were used for copper and iron quantification in thiocyanate-acetone medium (Kitson, 1950). One milliliter 37% HCl, 250 μL 3.5 M $(NH_4)_2S_2O_8$, and 13.75 mL of a 0.6 M NH_4SCN 90% acetone solution were added to 1 mL of sample aliquot and adjusted to 25 mL with distilled water. The absorbance of the thiocyanate-acetone mixture was measure at 380 and 480 nm within 10 min using a mixture without sample as the blank. The soluble metal concentrations were calculated according to Kitson (1950) and compared against standard curves prepared with $FeCl_3{\cdot}6H_2O$ and $CuCl_2{\cdot}2H_2O$.

Sample time points taken from the dissolution kinetic experiments with KCN were analyzed by capillary zone electrophoresis (Petre and Larachi, 2006; Petre et al., 2008). The samples were injected via hydrodynamic mode (10 cm height for 20 s) using a Waters (Milford, MA, USA) Ion Analyzer system equipped with a 95 cm fused-silica capillary (75 μm ID; Agilent Technologies, Santa Clara, CA, USA). A filtered (0.2 μm) and degassed 20 mM K_2HPO_4 pH 10, 1 mM KCN, 0.7 mM hexamethonium bromide solution was used as the carrier electrolyte. The capillary was conditioned daily before use with 0.1 M KOH for 30 min, and flushed between each sample run with the carrier electrolyte for 12 min. A 25 kV negative constant voltage (~68 μA) was applied for the separation, and the species were detected at 214 nm over a ~1 cm detection window in the capillary. Quantification of soluble copper, iron, and thiocyanate was made on the basis of cuprocyanide {$[Cu(CN)_3]^{2-}$}, ferrocyanide {$[Fe(CN)_6]^{4-}$}, ferricyanide {$[Fe(CN)_6]^{3-}$}, and SCN^- signals compared to standard solutions of CuCN, $K_3Fe(CN)_6$, $K_4Fe(CN)_6{\cdot}3H_2O$, and NaSCN (Sigma-Aldrich) dissolved in 0.1–3.0% KCN. Peak identity was verified by comparing the absorbance ratio of the signals at 214 and 254 nm to their corresponding standard solutions, and by comparing their migration time relative to an internal standard of $(NH_4)_6Mo_7O_{24}$. The Waters Millennium software was used for data acquisition and analysis.

3. Results

3.1. Hydrogen peroxide leaching of sulfides

The leaching capability of hydrogen peroxide (step 5 in the sequential extraction procedure of Dold, 2003a; Fig. 1; Table S1) was tested by a partial extraction of copper/iron sulfide concentrates using 35% H_2O_2 for 1 h at 80 °C. The dissolved metals after the partial extraction indicate that chalcocite was not dissolved, and that less than 10% of covellite was dissolved (Fig. 2). A comparable low solubility was obtained when treating enargite and bornite under hydrogen peroxide leaching. By contrast, pyrite and chalcopyrite samples showed a dissolution of over 50% based on the dissolved iron and copper, respectively (Fig. 2).

X-ray diffraction of the leaching residues compared to the sulfide minerals before treatment shows the precipitation of secondary minerals after hydrogen peroxide leaching of chalcocite, covellite, and bornite, indicating extensive metal redistribution among phases (Fig. 3;

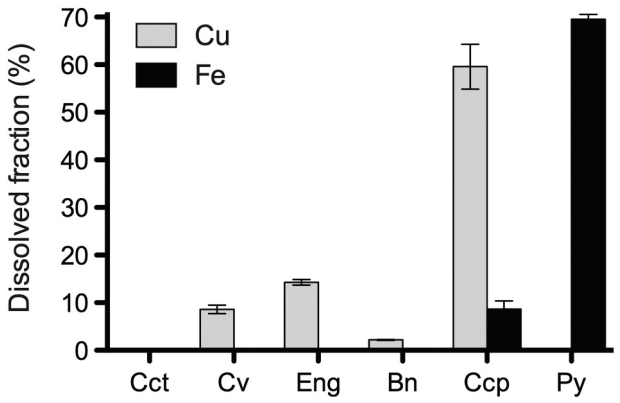

Fig. 2. Dissolution of sulfide concentrates using 35% hydrogen peroxide. Mineral dissolution is expressed as percentages of total Cu and Fe dissolved in triplicate samples using the fifth step of the sequential extraction described by Dold (2003a). Abbreviations after Whitney and Evans (2010): Cct, chalcocite; Cv, covellite; Eng, enargite; Bn, bornite; Ccp, chalcopyrite; Py, pyrite.

Table S2). For example, the chalcocite concentrate almost completely transformed into digenite (Fig. 3A). In addition, the chalcocite residue also contains copper oxides/oxyhydroxides precipitates, such as tenorite and posnjakite. Different precipitates are present in other leaching residues, such as brochantite in the case of covellite and bornite (Fig. 3B), barite in bornite (Fig. 3C), and sulfur after chalcopyrite leach (Fig. 3E).

3.2. Evaluation of acid oxidative leaching to selectively dissolve supergene sulfides

Supergene sulfides are preferentially dissolved by solutions of hydrochloric or sulfuric acid. However, the dissolution under acid leaching is considerably slow, unless the dissolution rates are increased by the addition of oxidizing agents, high temperature, and/or high pressure (e.g., Vračar et al., 2003; Descostes et al., 2004; Senanayake, 2009; Sokić et al., 2009; Velásquez-Yévenes et al., 2010; Miki et al., 2011; Xian et al., 2012). We evaluated the effects of H_2O_2, NO_3^-, and $P_2O_7^{4-}$ added as oxidizing agents in hydrochloric acid media to test their potential in selectively dissolving supergene sulfides.

The dissolution kinetics of chalcocite, chalcopyrite, and pyrite were evaluated using leaching solutions of 0.5 and 2 M HCl containing 0.1 or 0.5 M H_2O_2. Fig. 4 shows that, even though chalcocite rapidly and preferentially dissolves under either condition, its dissolution never reached more than 80% over the span of a two-hour reaction. Higher concentrations of both HCl and H_2O_2 did not promote higher dissolution rates for chalcocite, whereas chalcopyrite and pyrite dissolution increased (Fig. 4B). Alternative oxidizing agents (NO_3^- and $P_2O_7^{4-}$) also increased the dissolution rates of chalcopyrite and pyrite (Fig. S1). For all the dissolution experiments evaluated, increasing the concentration of oxidizing agents in the leaching solution had little effect to promoting the selective dissolution of chalcocite.

3.3. Evaluation of alkaline complexation to selectively dissolve supergene sulfides

Sulfide dissolution using ammonia or cyanide as complexing agents in alkaline solutions has also been evaluated to selectively dissolve secondary sulfides. Chalcocite preferentially dissolves in the presence of ammonia (Sarveswara Rao and Ray, 1998; Breuer et al., 2005). However, similarly to the acid oxidative leaching conditions (Section 3.2), ammonia solutions did not completely dissolve chalcocite. Addition of oxidizing agents to promote chalcocite dissolution (0.1 M ammonium persulfate in 3.0 M NH_3; Liu et al., 2012) also increased copper dissolution from chalcopyrite, therefore failing to differentiate supergene from hypogene sulfide minerals (Fig. S2).

By contrast, cyanide is a strong metal complexing agent that promotes reducing conditions during sulfide leaching (Petre and Larachi, 2006; Petre et al., 2008). To determine the efficiency of cyanide for sulfide dissolution, the sulfide concentrates were evaluated by dissolution kinetic analyses using alkaline solutions of potassium cyanide ranging from 0.1 to 3.0%. Chalcocite and covellite were completely dissolved within the first 15 min of leaching using KCN concentrations over 0.5% (Fig. 5). Copper dissolution from the cyanidation of chalcopyrite reached ~10% within the first 15 min, whereas virtually no dissolution of pyrite was observed when treated with 0.5% KCN (Fig. 5). Dissolution rates of enargite and bornite under cyanidation were higher than chalcopyrite, but lower than the supergene sulfides. Overall, the cyanidation of sulfide concentrates showed a dissolution tendency in the order of Cct > Cv > Eng > Bn > Ccp > Py, where selective dissolution of supergene sulfides is achieved within 10–15 min of leaching with 0.5% KCN.

3.4. Cyanide leaching in the sequential extraction of tailings impoundment samples

The dissolution of supergene sulfides by cyanide was tested as part of the sequential extraction scheme proposed by Dold (2003a). Samples from the neutralization and the primary sulfide zones of the La Andina porphyry copper mine tailings impoundments were either extracted by using a fifth dissolution step with hydrogen peroxide for 1 h (Fig. 1; Table S1), or by replacing the fifth step using a 0.5% potassium cyanide leach (Fig. 6; Table S3).

Comparison of the two extraction methods reveals that hydrogen peroxide solubilized more copper than cyanide for all the samples analyzed (Fig. 6A). Iron dissolution was also higher when hydrogen peroxide was used for the extraction. Fig. 6B shows that iron remained largely undissolved during the cyanide treatment compared to hydrogen peroxide when used as the fifth step of the sequential extraction.

The reaction products during the cyanidation of the tailings were also visualized at different time points by capillary electrophoresis throughout the dissolution progression. Fig. 7A shows the dissolution kinetics of copper, iron, and thiocyanate during the cyanide leaching used as the fifth step of the sequential extraction applied to representative tailings samples from the neutralization and the primary zones. Copper extraction reached a plateau after ~10 min of reaction. Fig. 7B shows the electropherograms of the dissolution of a tailings sample with 0.5% KCN at different time points, where changes in the different redox couples are visualized through time.

4. Discussions

4.1. The effect of hydrogen peroxide leaching on copper iron sulfides

The hydrogen peroxide leaching in the seven-step sequential extraction applied by Dold (2003a) showed a limited selectivity to dissolve secondary sulfide minerals. When mixed with sulfides, a 35% hydrogen peroxide solution produces an exothermic, usually violent, reaction. The reaction also produces visible fumes, possibly containing SO_2 (Fig. S3). In addition to the difficulties associated with the manipulation of highly exothermic reactions, the potential volatilization of SO_2 would prevent a mineralogical estimation on the basis of dissolved sulfur. Previous sequential extraction data using hydrogen peroxide leaching showed considerable sulfur loss, possibly via SO_2 volatilization (unpublished data). In addition, supergene sulfides are not effectively dissolved by hydrogen peroxide treatment (Fig. 2), and these conditions also facilitate the precipitation of other sulfides and oxides (Fig. 3; Table S2), increasing the complexity of the system by element remobilization among the sequential extraction steps.

After H_2O_2 digestion, the chalcocite concentrate transforms into digenite (Fig. 3A). Digenite normally occurs as a weathered form of chalcocite (Jennings et al., 2000). Hydrogen peroxide treatment could

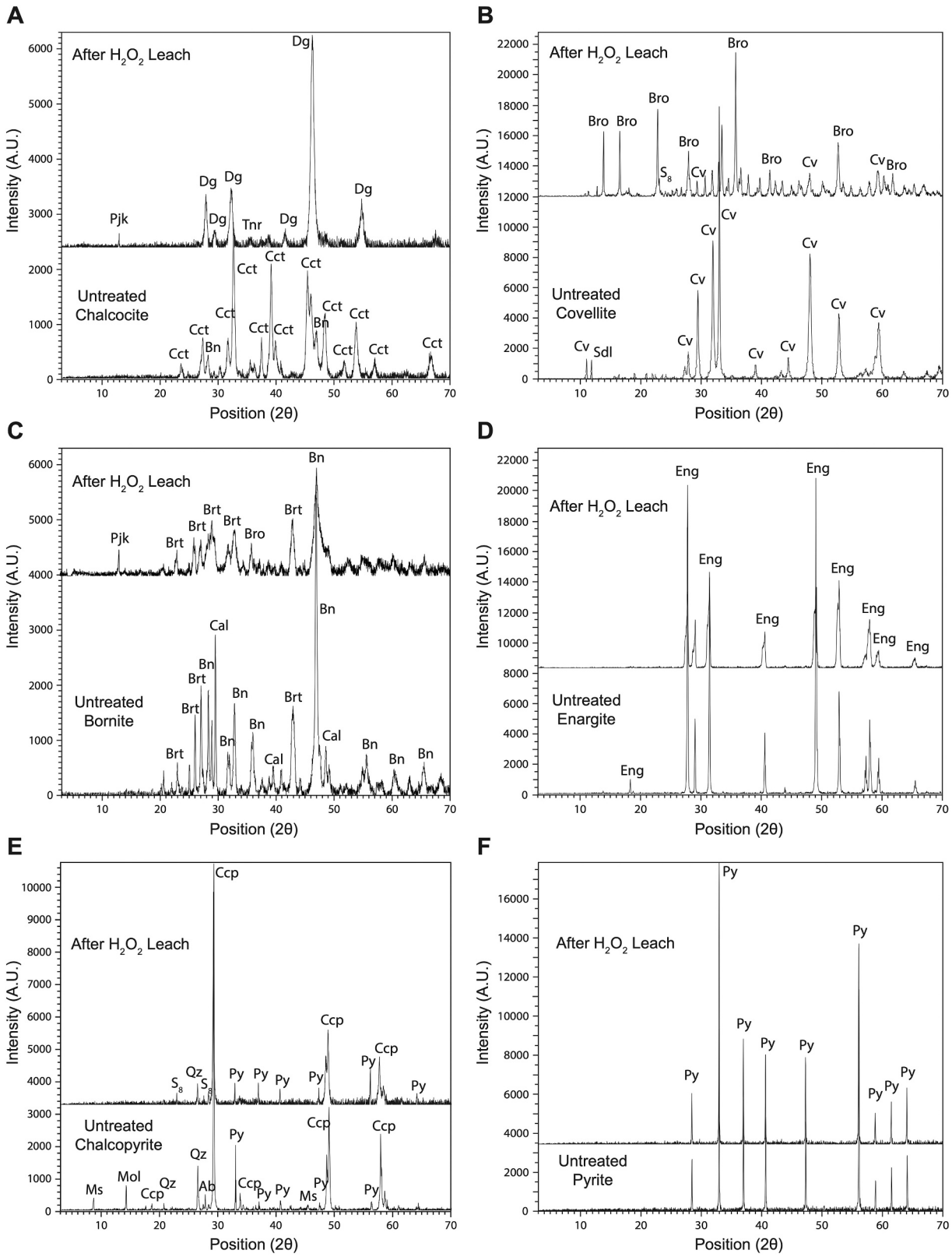

Fig. 3. X-ray diffraction of the sulfide concentrates and their residues after hydrogen peroxide leaching. The lower diffractograms on each panel correspond to the chalcocite (A), covellite (B), bornite (C), enargite (D), chalcopyrite (E), and pyrite (F) samples prior to hydrogen peroxide leaching. The upper diffractograms correspond to their residues after 35% H_2O_2 treatment. Abbreviations after Whitney and Evans (2010): Ab, Ca-rich albite; Brt, barite; Bn, bornite; Bro, brochantite; Cal, calcite; Cct, chalcocite; Ccp, chalcopyrite; Cv, covellite; Dg, digenite; Eng, enargite; Mol, molybdenite; Ms, muscovite; Pjk, posnjakite; Py, pyrite; Qz, quartz; S_8, sulfur (octathiocane); Sdl, sodalite; Tnr, tenorite.

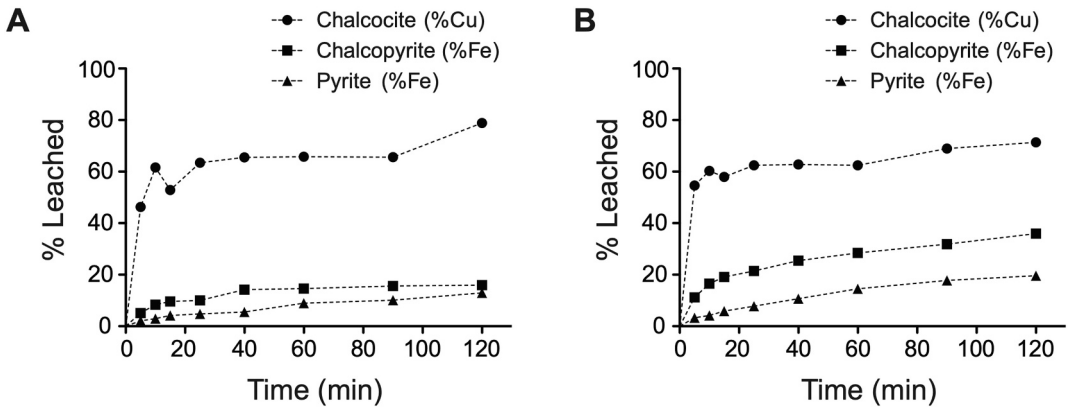

Fig. 4. Dissolution kinetics of chalcocite, chalcopyrite, and pyrite concentrates under acid oxidative conditions. (A) 0.5 M HCl, 0.1 M H_2O_2. (B) 2.0 M HCl, 0.5 M H_2O_2. Dissolution values are expressed as the percentage of dissolved copper from chalcocite, or dissolved iron from chalcopyrite or pyrite compared to the total copper/iron content in each sample.

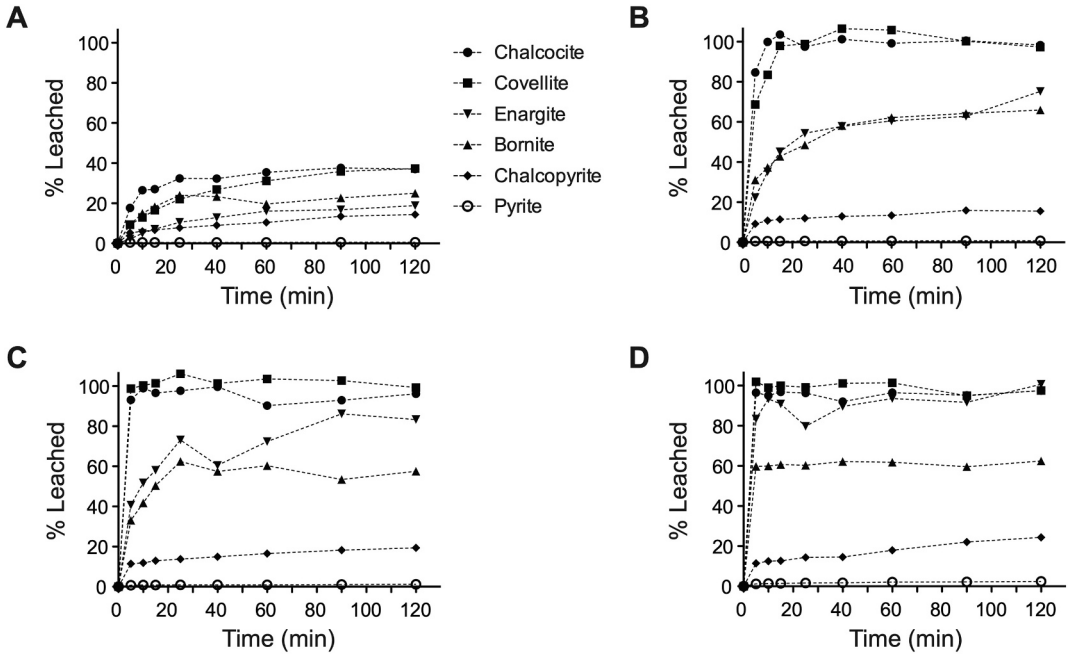

Fig. 5. Dissolution kinetics of sulfide concentrates under cyanidation. Dissolution progression at different time points using 0.1% (A), 0.5% (B), 1.0% (C), or 3.0% (D) KCN. Values are expressed as the percentage of leached copper from the concentrates of chalcocite (circle), covellite (square), enargite (inverted triangle), bornite (triangle), and chalcopyrite (diamond), or expressed as the percentage of leached iron from pyrite (open circle), compared to the total copper/iron content in each mineral.

emulate the relatively slower oxidation of chalcocite by water and atmospheric oxygen, leading to the formation of digenite (Jennings et al., 2000; Miki et al., 2011). Two different mechanisms may be involved in chalcocite transformation: re-precipitation of the dissolved elements to form digenite, or direct transformation of the crystal lattice. Transformation of the crystal lattice could be associated with the oxidative progression during dissolution of chalcocite. According to a proposed leaching mechanism in acid oxidative conditions, chalcocite dissolves through different steps that lead to the formation of sulfides with progressively less copper, from chalcocite (Cu_2S) to djurleite ($Cu_{1.94}S$), digenite ($Cu_{1.8}S$), and finally covellite (CuS) (Elsherief et al., 1995; Arce and González, 2002; Miki et al., 2011). The oxidation of chalcocite to digenite is described by the following oxidation half-reaction (Eq. (1)):

$$Cu_2S_{(s)} \rightarrow Cu_{1.8}S_{(s)} + 0.2Cu^{2+} + 0.4e^- \quad (1)$$

When coupled to hydrogen peroxide as the electron acceptor, the overall reaction is (Eq. (2)):

$$2Cu_2S_{(s)} + H_2O_{2(aq)} + 2H^+{}_{(aq)} \rightarrow 5Cu_{1.8}S_{(s)} + Cu^{2+}{}_{(aq)} + 2H_2O_{(l)} \quad (2)$$

According to the stoichiometry of chalcocite oxidation to digenite by hydrogen peroxide (Eq. (2)), the molar excess of hydrogen peroxide in the leaching medium used to dissolve chalcocite in Fig. 3A is approximately 18 times above the equimolar quantity required for the complete oxidation of chalcocite to digenite. Therefore, the amount of hydrogen peroxide used was sufficient to explain the entire transformation observed in Fig. 3A, where no chalcocite (nor djurleite) was found in the residue.

In addition, copper oxide precipitates (tenorite and posnjakite) were found in the residue of chalcocite leaching (Fig. 3A). Secondary oxide precipitates have also been found in previous reports of chalcocite leaching with hydrogen peroxide (Jennings et al., 2000). Furthermore, the precipitation of oxides could form passivation layers on the sulfide

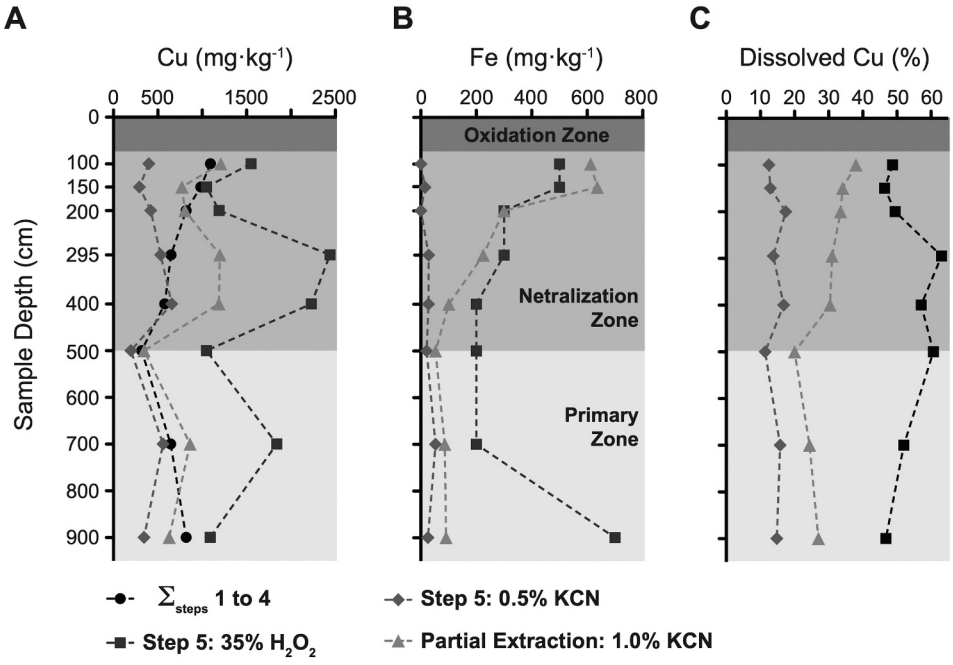

Fig. 6. Comparison of cyanide and hydrogen peroxide leaching in the sequential extraction of samples from porphyry copper tailings. Each curve represents the amount of dissolved copper (A), iron (B), or copper as a percentage of total copper in the samples (C) recovered from the sequential extraction steps one to four (the summation of all four steps is shown), a partial extraction (with no previous dissolution steps) using 1.0% KCN, and the fifth step of the sequential extraction using either 35% hydrogen peroxide or 0.5% potassium cyanide for 1 h as a function of sample depth.

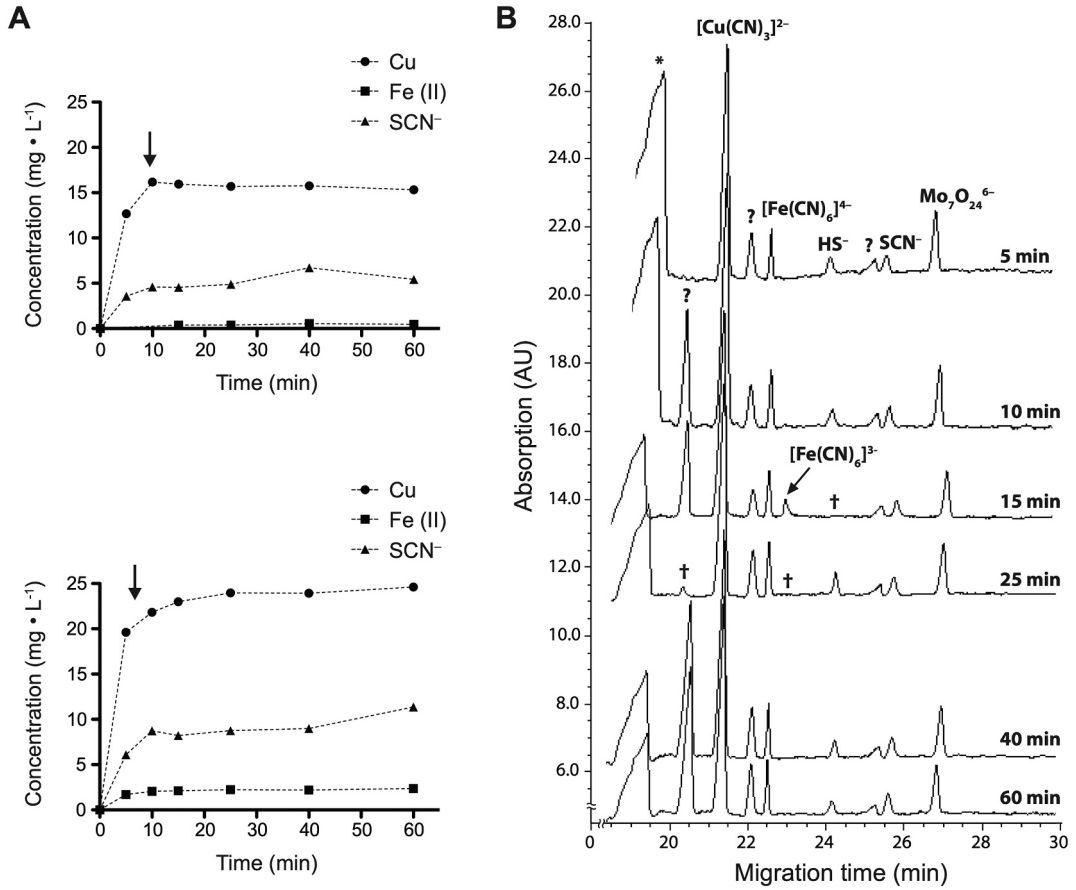

Fig. 7. Dissolution kinetics of porphyry copper tailings samples under cyanidation. (A) Dissolved copper, iron, and thiocyanate from representative samples taken at the neutralization (upper panel) and the primary zone (lower panel) using 0.5% KCN as the fifth step of the sequential extraction proposed by Dold (2003a). Arrows indicate the approximate time at which the rate of copper dissolution changed. (B) Electropherograms of the tailings sample taken at 7 m depth throughout the dissolution progression shown in A. The peaks are identified as cuprocyanide $\{[Cu(CN)_3]^{2-}\}$, ferrocyanide $\{[Fe(CN)_6]^{4-}\}$, ferricyanide $\{[Fe(CN)_6]^{3-}\}$, hydrosulfide (HS^-), thiocyanate (SCN^-), and heptamolybdate ($Mo_7O_{24}^{6-}$; internal standard) anions. Unidentified peaks are indicated with a question mark (?), and signal disappearance relative to the preceding time point are shown with a cross (†). The arrow indicates the appearance of ferricyanide $\{[Fe(CN)_6]^{3-}\}$ complex at 15 min of leaching. *Peak of the system.

surfaces, preventing further oxidation of digenite to covellite and, ultimately, preventing its complete dissolution. The overall reaction of chalcocite with hydrogen peroxide involving the formation of tenorite and digenite is represented as follow (Eq. (3)):

$$2Cu_2S_{(s)} + H_2O_{2(aq)} \rightarrow 5Cu_{1.8}S_{(s)} + CuO_{(s)} + 2H_2O_{(l)} \quad (3)$$

Tenorite, as well as posnjakite and other oxides found after the hydrogen peroxide leaching, precipitate as a consequence of the exposure to oxidizing agents. The precipitation of brochantite observed in the covellite and bornite residues after hydrogen peroxide treatment may also represent oxidative sulfide weathering, emulating atmospheric oxygen in natural environments, as well as supergene enrichment in porphyry copper deposits (Fig. 3B, C; Pinget, 2016).

A non-stoichiometric relationship is also observed in the copper and iron concentrations obtained after hydrogen peroxide treatment of chalcopyrite (Fig. 2). The higher solubility of copper relative to iron may be explained by the reprecipitation of iron into poorly crystalline ferrihydrite/schwertmannite phases, which cannot be detected through standard X-ray diffraction techniques (Fig. 3E). After H_2O_2 treatment, iron oxide precipitation on chalcopyrite samples was observed by a color change from dark gray (the color of the sulfide concentrate before treatment), to reddish-brown (the color of the residue after hydrogen peroxide treatment). Iron oxide/oxyhydroxides might be represented by humps at 35 and 62 2θ position in the diffractogram of Fig. 3E. Given the possible formation of precipitates, iron from chalcopyrite potentially redistributes to the next step of a sequential extraction procedure when hydrogen peroxide leaching is used. The precipitation of secondary oxides could also form a passivation layer on sulfide grains, preventing further dissolution of chalcopyrite under oxidizing conditions (e.g., Córdoba et al., 2008a, 2008b). A passivation layer may also be formed by the precipitation of sulfur. Sulfur precipitates are observed after the H_2O_2 leaching of covellite and chalcopyrite concentrates (Fig. 3B, E), in agreement with previous findings of sulfur precipitation on chalcopyrite and other sulfide surfaces under acid oxidative leaching (Córdoba et al., 2008a, 2008b; Nicol et al., 2010).

In addition to sulfide passivation by secondary precipitates, it is also possible that the composition of the sample could facilitate mineral dissolution during hydrogen peroxide leaching. Transition metals, such as ferrous and ferric ions, may catalyze the generation of free radicals from hydrogen peroxide. Hydroxyl ($OH^{\bullet}$), superoxide ($O_2^{\bullet -}$), perhydroxyl ($HO_2^{\bullet}$), and ferryl (FeO^{2+}) radicals can be formed by the Fenton reaction, which may enhance the oxidative dissolution of sulfides (Teel et al., 2007; Ruiz-Sánchez and Lapidus, 2017). Radical generation may explain the relatively high metal dissolution from iron-containing minerals under hydrogen peroxide treatment (Fig. 2). Parallel reactions (such as radical formation) may constitute an important mechanism on the effect of accessory minerals over the dissolution rate of copper sulfides (Lundström et al., 2012). For example, the presence of pyrite has been shown to enhance the dissolution rates of chalcopyrite and covellite under acid oxidative conditions (Nicol et al., 2010; Velásquez-Yévenes et al., 2010; Miki et al., 2011). In theory, it is possible to increase the dissolution of secondary sulfides by mixing them with acid-producing primary sulfides. The dissolution of chalcopyrite and pyrite with hydrogen peroxide produces acidity, whereas the dissolution of chalcocite and covellite does not. The released acidity by chalcopyrite and/or pyrite would further promote chalcocite and covellite dissolution, thereby facilitating the heterogeneous dissolution of secondary sulfides (conditional to the matrix of each sample), which ultimately precludes their selective dissolution.

4.2. The effect of acid oxidative leaching of sulfides

Even though supergene sulfides dissolve faster under acid media compared to chalcopyrite and pyrite, the dissolution rates obtained in this study (Fig. 4; Fig. S1) are not sufficient to differentiate among chalcocite, chalcopyrite, and pyrite based on their dissolved elements. Therefore, incorporation of an acid oxidative dissolution step would also fail as the fifth step of the sequential extraction procedure proposed by Dold (2003a). Increased concentrations of hydrogen peroxide in hydrochloric acid media showed a little effect on copper recovery from chalcocite, which instead favored the dissolution of primary minerals (Fig. 4), in agreement with previous theoretical and experimental evidence (Córdoba et al., 2008a; Nicol et al., 2010). The dissolution tendency under acid oxidative conditions was always in the order Cct > Ccp > Py, in agreement with previous experimental dissolution data (e.g., Vračar et al., 2003; Descostes et al., 2004; Senanayake, 2009; Sokić et al., 2009; Velásquez-Yévenes et al., 2010; Xian et al., 2012). Despite the preferential leaching of chalcocite (~60% in Fig. 4), the partial dissolution of chalcopyrite and pyrite can potentially obscure the differentiation among these phases in a hypothetical sequential extraction scheme. Based on these results, it is therefore not recommended to discriminate supergene from hypogene sulfide minerals on the basis of their dissolution rates using acid oxidative conditions.

4.3. Selective dissolution of supergene copper sulfides by cyanidation

Among complexing agents, cyanide has shown to entirely dissolve chalcocite within minutes (Fisher et al., 1992; Fisher, 1994; Breuer et al., 2005). The dissolution mechanism of chalcocite in the presence of cyanide proceeds via copper complexation under non-oxidative conditions, represented by the following equation (Eq. (4)):

$$Cu_2S_{(s)} + 2nCN^-_{(aq)} \rightarrow 2\left[Cu(CN)_{(n)}\right]^{(n-1)-} + S^{2-}; \text{ where } n = 1; 2 \text{ or } 3 \quad (4)$$

As shown in Fig. 4, oxidizing conditions favor the leaching of chalcopyrite and pyrite (Córdoba et al., 2008a; Nicol et al., 2010). Therefore, a non-oxidative dissolution mechanism, such as the cyanide complexation shown in Eq. (4), has the potential to limit the dissolution of primary sulfide minerals, which proves useful for sulfide estimation based on selective dissolution. The redox state of the species quantified in this study by capillary electrophoresis further illustrate the reducing conditions during the cyanidation of sulfides. As a result, the dissolution of chalcopyrite and pyrite under cyanide treatment is reduced (Fig. 5). In addition, the high stability constant of copper/iron-cyano complexes facilitates rapid metal sequestration, preventing the potential oxidation of sulfides by the release of cupric or ferric ions into the solution. Released oxidized species are important to take into consideration during sulfide leaching. Cupric and/or ferric ions released as by-products of chalcopyrite and pyrite dissolution can provide oxidative potential that is otherwise absent in the leaching medium (Córdoba et al., 2008a).

It is also important to note that differences in the sample composition could potentially lead to mineralogical misinterpretations. Chalcopyrite and pyrite show a reduced dissolution rate under cyanidation, which facilitates their mineralogical interpretation on the basis of dissolved copper and iron when compared to chalcocite and covellite in sulfide-containing samples (Fig. 5). The presence of other minerals, however, can potentially confound estimates of chalcocite. For example, enargite and bornite have higher dissolution rates compared to chalcopyrite and pyrite (Fig. 5). Within a few minutes, copper recovery from enargite and bornite reached over 30% using KCN concentrations of 0.5% or higher. Even though it is possible to differentiate enargite and bornite on the basis of arsenic and iron dissolution on a sequential extraction procedure, other arsenic- and iron-bearing sulfides not evaluated in this study, such as tennantite, arsenopyrite and/or pyrrhotite among others, could interfere as well.

4.4. Cyanide leaching in the sequential extraction of tailings samples

When applied as the fifth step of the sequential extraction method after Dold (2003a), cyanide leaching better reflects the mineralogy of

tailings samples compared to the 35% hydrogen peroxide leaching. Comparison of both extraction procedures reveals that hydrogen peroxide treatment typically solubilizes between three- to five-fold more copper than cyanide leaching (Fig. 6A). Giving the low recovery of copper from the chalcocite concentrate under H_2O_2 leaching (Fig. 2), higher copper recoveries obtained after H_2O_2 leaching of the tailings samples are possibly associated with non-selective dissolution of primary sulfides, such as chalcopyrite. If hydrogen peroxide selectively dissolves supergene sulfides, then between 45 and 65% of the total copper in the tailings samples can be interpreted to derive from secondary sulfides (Fig. 6C). Yet, chalcopyrite is the main copper sulfide mineral, with only minor supergene replacement at the neutralization zone observed in these tailings samples (Dold and Fontboté, 2001). By contrast, less than 20% of the total copper was solubilized when 0.5% KCN was used instead of the 35% H_2O_2 as the fifth step of the sequential extraction (Fig. 6C). In addition, the dissolution kinetics of copper during cyanidation of the tailings samples agree with the kinetic patterns of secondary and primary sulfide leaching. Fig. 7A shows a rapid increase in copper dissolution from the tailings within the first 5–10 min of leaching, which could possibly be associated with the dissolution of secondary sulfides, such as chalcocite and covellite. Changes in the copper dissolution rates after 5–10 min (arrows in Fig. 7A) presumably correspond to the leaching of chalcopyrite.

Iron dissolution from the tailings samples is also higher when hydrogen peroxide is used as the fifth step of the sequential extraction (Fig. 6B). In addition, dissolved iron is three- to 30-fold higher than copper. This variability could be explained by the heterogeneity of the samples analyzed. Other metal bearing sulfides in the tailings samples could act as catalysts for the oxidation reaction promoted by hydrogen peroxide, or could release complexing agents (such as chloride, chlorate, or sulfate) into the solution, increasing the solubility of metals and leading to a potential misinterpretation of the data. Therefore, cyanide leaching was more reliable than hydrogen peroxide treatment for the dissolution of copper sulfide-bearing tailings samples.

All of the cyanide tailings leachates revealed unidentified reaction products, including the appearance and disappearance of certain peaks throughout the dissolution progression visualized by capillary electrophoresis over time. For example, in Fig. 7B, a peak at 20.5 min migration time is observed in the leachate analyzed at 10 min, then it disappeared in the sample taken after 25 min of leaching, and appeared again after 40 min. A similar pattern is observed in all the tailings samples analyzed. It is possible that the formation and consumption of unidentified species is governed by the redox equilibrium of the system during cyanidation. Some solubilized species are redox sensitive, and their redox state change according to the reduction potential of the leachate (Petre and Larachi, 2006; Petre et al., 2008). The unidentified peaks in Fig. 7B could also correspond to polysulfide intermediates (Hewitt et al., 2009). Sulfide dissolution may release polysulfide species into the reaction medium, which can further react with cyanide to produce thiocyanate and hydrosulfide according to the Eq. (5) (Breuer et al., 2008):

$$S_x^{2-} + (x-1)CN^- \rightarrow (x-1)SCN^- + S^{2-} \quad (5)$$

Both products of Eq. (5) were identified by capillary electrophoresis, where the formation kinetics of thiocyanate may represent the overall sulfide dissolution progression (Fig. 7A). Furthermore, a redox change involving known species is visualized in the electropherogram from the sample taken at 15 min of leaching (Fig. 7B). The emergence of a peak corresponding to ferricyanide follows the disappearance of the hydrosulfide peak. The released hydrosulfide has the potential to reduce ferric ion (Piché and Larachi, 2007; Petre et al., 2008), therefore, ferricyanide possibly overcame the hydrosulfide equivalents at 15 min of leaching. Once the reaction proceeded (25 min in Fig. 7B), additional hydrosulfide ions released into the solution potentially reduced ferricyanide to ferrocyanide. Iron reduction is visualized by the substitution of the ferricyanide peak by a hydrosulfide peak. The redox pattern observed throughout the dissolution progression in Fig. 7B shows that reducing conditions (relative to the ferro/ferricyanide redox couple) govern the cyanide leaching media, which ultimately minimizes the dissolution of primary sulfides.

In addition to the sequential extraction using 0.5% KCN as the fifth step, the tailings samples were also directly treated with 1.0% KCN, without previous leaching steps (partial extraction data in Fig. 6). It is generally assumed that the conditions used in a sequential extraction step are more abrasive than the previous step, increasing the order of aggressiveness throughout the sequence (Sutherland, 2010). In the case of cyanidation, however, the 1.0% KCN solution may not completely dissolve oxide phases in the samples. The effect of the preceding steps of the sequential extraction can be observed by comparing the 1.0% KCN 1 h partial extraction of the tailings samples with the total copper recoveries from the steps 1, 2, 3, and 4 of the sequential extraction (Fig. 6). The overall copper extracted by partial extractions was higher than the copper obtained by cyanidation in the sequential scheme; however, in some samples, the copper recovered by the partial extraction was less than the total amount of copper leached by all the first four steps of the sequential extraction, suggesting that cyanidation, even at a higher concentration and time, does not always dissolve the expected quantity of copper by partial extraction. The matrix effect in these samples is also relevant, because the presence of other cyanide-complexing metals could interfere with the availability of free cyanide in solution (e.g., Oraby and Eksteen, 2014; Oraby et al., 2017; Barani et al., 2021). In addition, it is possible that oxide coatings form passivation layers on sulfide minerals, preventing their leaching by cyanide. Oxide coatings are expected to dissolve in the previous leaching steps of a sequential extraction scheme, which provides a cleaner reaction surface for the cyanide attack. Therefore, previous steps of the sequential extraction (Fig. 1; Table S1) may be required for the selective dissolution of supergene sulfides in the tailings samples analyzed.

Although not evaluated in this study, the presence of other copper-containing minerals, such as supergene copper oxides at the neutralization zone of the tailings impoundment, could potentially be dissolved by the partial extractions using cyanide (Fig. 6). Copper oxides are also an important source of copper (e.g., Zhang et al., 2021a, 2021b; Wang et al., 2021), some of which can partially dissolve under cyanidation (e.g., Breuer et al., 2005; Oraby et al., 2017; Barton et al., 2018). The higher recoveries of copper (and iron) by the 1.0% KCN partial extraction compared to the cyanide treatment as the fifth step of the sequential extraction (Fig. 6) are possibly associated with the dissolution of copper oxides in the tailings samples. Therefore, cyanide leaching at different levels of a sequential extraction scheme could potentially be used to estimate the mineralogy of copper oxides.

4.5. Applications of selective dissolutions for mineralogical interpretations

The selective dissolution strategy described in this study has the potential to complement existing mineralogical techniques to better quantify the mineralogy of a sample. Its applicability, however, relies on the presence of other sulfide minerals not analyzed in this study, the variable solubility of copper/iron sulfides from different ore deposits, and the presence of accessory minerals in the sample matrix. Ideally, selective dissolution techniques should be calibrated according to the mineralogy of the particular ore deposit in study (e.g., Dold, 2003a, 2003b; Preece et al., 2018). When reliable, a sequential extraction of sulfides can provide two immediate applications in the mining industry: increasing the predictability of the selected metallurgical approach, and obtaining a detailed acid-base accounting for the prediction of AMD and associated trace element release.

The mineralogy of the ore ultimately defines the material sorting for metallurgical operations (e.g., Scheffel et al., 2016; Barton et al., 2018; Bicak, 2019; Bahrami et al., 2021). In the mining of porphyry copper ores, the deposit is usually divided into metallurgical units that have three different destinations: waste dumps, heap bioleaching of leachable

supergene minerals, or flotation and smelting of hypogene sulfides (Dold, 2010; Dold and Weibel, 2013). Sulfide evaluation is fundamental to optimize the exploitation processes because different copper-bearing minerals have different metallurgical behavior (Jacques et al., 2016). Large-scale estimates of sulfide mineral loads are, however, usually performed via visual assessment of core drill samples. Depending on mineral zonation, petrographic microscopy and chemical quantification of acid-soluble and total copper are also evaluated. Additional quantification by automated mineralogy has been successfully implemented by techniques such as mineral liberation analysis (MLA) and quantitative evaluation of minerals by scanning electron microscopy (QEMSCAN®; Dold, 2017; Guanira et al., 2020). Automated techniques have, however, some disadvantages. A detailed calibration of the specific ore deposit by X-ray diffraction and petrographic microscopy is usually required in addition to the automated analysis, which substantially increases analytical costs. Higher costs reduce the analyses to fewer samples, therefore, the quality of the data highly relies on the sample representativeness and the heterogeneity of the deposit. In addition, biases associated with differential segregation of mineral grains during the elaboration of briquettes required for automated analyses are usually observed (Pooler and Dold, 2017).

To overcome inaccuracies in mineralogical estimates, detailed chemical analysis via sequential extractions can provide a cost- and time-effective methodology to quantify the assemblage of sulfide minerals in ore deposits. A sequential extraction-based quantification of sulfides proves particularly useful for the estimation of mineral types in transition zones. Differentiating between supergene and primary sulfide minerals via sequential extraction allows a characterization of the mineral assemblage that is required to sort sulfides to either heap leaching or froth flotation. Chemical analyses are cheaper (therefore, more samples can be evaluated) and faster than other mineralogical techniques. In addition, chemical evaluation of leaching solutions provides lower detection limits for the analysis of trace elements. A rapid and simple mineralogical characterization technique can also be applied in the field during mineral extraction. Daily testing of sulfides in the blasting site increases the predictive value of mining operations by evaluating the agreement of each metallurgical unit with the mid- and long-term geometallurgical model, minimizing potential failures in downstream operations (Dold and Weibel, 2013).

Accurate mineralogical interpretations are also required for the calculation of an acid-base accounting that better reflects the potential for AMD generation (Dold, 2017). Sequential extraction data can be used to differentiate the different contributions of potential acid release by primary and secondary sulfide minerals (Dold and Weibel, 2013; Blowes et al., 2014). Traditionally, the acid-base accounting is performed by considering the oxidation potential of total sulfur as pyrite, which generates 2 mol of protons per mole of sulfur. However, different sulfide minerals have different potential to generate acidity. Chalcopyrite generates only 1 mol of protons per mole of sulfur, whereas chalcocite and covellite do not generate acidity. Differential acidity contributions should be considered for the accurate prediction of AMD release potential in ore deposits containing a complex sulfide assemblage. When adapted to the solubility of specific sulfides in the ore body, sequential extraction procedures have the potential to increase the sustainability of mining operations by the calculation of a high-resolution acid-base accounting (Dold, 2008; Dold and Weibel, 2013).

Sulfide interpretation using selective dissolution techniques also has the potential to evaluate the re-processing of old mining tailings. Several sulfidic tailings from old porphyry copper operations contain copper at higher concentrations than the current cut-off ore grades (Alcalde et al., 2018). However, tailings deposits (especially the tailings derived from old mining activities) likely have extensive sulfide oxidation and supergene enrichment (Dold and Fontboté, 2001). In this particular scenario, sequential extractions provide several advantages compared to other mineralogical techniques. Microscopic evaluation of tailings samples is challenging, because the material is already crushed and milled, which requires the preparation of briquettes that in turn increases the costs and the heterogeneity of the samples by differential segregation of minerals (Pooler and Dold, 2017). On the other hand, XRD analyses of tailings samples are limited, because the concentrations of sulfides in some tailings impoundments are usually lower than XRD detection limits. Therefore, mineralogical interpretations based on chemical extraction assays are convenient to define the metallurgical approach and to evaluate the environmental impact of the potential re-processing of old tailings.

5. Conclusions

Selective extraction of supergene sulfide minerals provides a plausible strategy to quantify the sulfide fraction in ore deposits. This study shows that adding a cyanidation step in a previously proposed sequential extraction procedure offers an alternative method to quantify copper/iron sulfide minerals on the basis of dissolved elements. Differences in the dissolution rates between secondary and primary sulfides under cyanidation (0.5% KCN, 5–10 min) enable an effective interpretation of the sulfide fraction. Incorporation of a cyanidation step in sequential extractions of sulfidic samples increased the selectivity to differentiate between the main supergene and hypogene sulfide minerals in supergene enriched copper sulfide ores, such as porphyry copper deposits. Consequently, if the selective dissolution of supergene copper sulfides is relevant for the study site, a cyanidation step is suggested to replace the hydrogen peroxide leaching in the fifth step of the sequential extraction described by Dold (2003a).

The selective dissolution of sulfides could complement other methods of mineral evaluation to thoroughly characterize the mineralogical assemblage of ore bodies, providing a fast, simple, and low-cost technique for the assessment of primary and secondary copper sulfide minerals. Ultimately, a cyanidation step incorporated in a sequential extraction can help provide a detailed understanding of the spatial distribution of sulfides in ore bodies, which proves essential for resource estimation, mineral sorting during metallurgical operations, and improving the copper recoveries and sustainability of the mining process.

CRediT authorship contribution statement

Fernando Medina Ferrer: Conceptualization, Methodology, Validation, Formal analysis, Investigation, Resources, Writing – Original Draft, Writing – Review & Editing, Visualization, Supervision, Project administration; **Bernhard Dold**: Conceptualization, Resources, Writing – Review & Editing, Supervision; **Oscar Jerez**: Resources, Writing – Review & Editing.

Declaration of competing interest

The authors declare that they have no known competing financial interests or personal relationships that could have appeared to influence the work reported in this paper.

Acknowledgements

FMF thanks Leyla Weibel and Robert Pooler for critical discussions and helpful suggestions, María Paz Ramírez, Andrés Ibarra, and Javier García Barriocanal for analysis assistance, Ashley Breiland and Daniel Jones for critical proofreading, and especially to María Antonieta Valenzuela for providing critical laboratory space and the capillary electrophoresis facility at the Department of Biochemistry and Molecular Biology, University of Chile. We are also grateful for the anonymous reviewers that helped increase the quality of this manuscript. FMF was funded by a master fellowship CONICYT-PCHA/MagísterNacional/2012 – folio 22120447.

Funding

This research did not receive any specific grant from funding agencies in the public, commercial, or not-for-profit sectors.

Appendix A. Supplementary data

Supplementary data to this article can be found online at https://doi.org/10.1016/j.gexplo.2021.106848.

References

Abrosimova, N., Gaskova, O., Loshkareva, A., Edelev, A., Bortnikova, S., 2015. Assessment of the acid mine drainage potential of waste rocks at the Ak-Sug porphyry Cu–Mo deposit. J. Geochem. Explor. 157, 1–14. https://doi.org/10.1016/j.gexplo.2015.05.009.

Alcalde, J., Kelm, U., Vergara, D., 2018. Historical assessment of metal recovery potential from old mine tailings: a study case for porphyry copper tailings, Chile. Miner. Eng. 127, 334–338. https://doi.org/10.1016/j.mineng.2018.04.022.

Arce, E.M., González, I., 2002. A comparative study of electrochemical behavior of chalcopyrite, chalcocite and bornite in sulfuric acid solution. Int. J. Miner. Process. 67, 17–28. https://doi.org/10.1016/S0301-7516(02)00003-0.

Bahrami, A., Ghorbani, Y., Sharif, J.A., Kazemi, F., Abdollahi, M., Salahshur, A., Danesh, A., 2021. A geometallurgical study of flotation performance in supergene and hypogene zones of Sungun copper deposit. Miner. Process Extr. Metall. 130, 126–135. https://doi.org/10.1080/25726641.2019.1591794.

Barani, K., Dehghani, M., Azadi, M.R., Karrech, A., 2021. Leaching of a polymetal gold ore and reducing cyanide consumption using cyanide-glycine solutions. Miner. Eng. 163, 106802.

Barton, I., Ahn, J., Lee, J., 2018. Mineralogical and metallurgical study of supergene ores of the Mike Cu–Au(–Zn) deposit, Carlin trend, Nevada. Hydrometallurgy 176, 176–191. https://doi.org/10.1016/j.hydromet.2018.01.022.

Bicak, O., 2019. A technique to determine ore variability in a sulphide ore. Miner. Eng. 142, 105927 https://doi.org/10.1016/j.mineng.2019.105927.

Blowes, D.W., Ptacek, C.J., Jambor, J.L., Weisener, C.G., Paktunc, D., Gould, W.D., Johnson, D.B., 2014. The geochemistry of acid mine drainage. In: Reference Module in Earth Systems and Environmental SciencesTreatise on Geochemistry, Second edition, 11, pp. 131–190. https://doi.org/10.1016/B978-0-08-095975-7.00905-0.

Breuer, P.L., Dai, X., Jeffrey, M.I., 2005. Leaching of gold and copper minerals in cyanide deficient copper solutions. Hydrometallurgy 78, 156–165. https://doi.org/10.1016/j.hydromet.2005.02.004.

Breuer, P.L., Jeffrey, M.I., Hewitt, D.M., 2008. Mechanisms of sulfide ion oxidation during cyanidation. Part I: the effect of lead(II) ions. Miner. Eng. 21, 579–586. https://doi.org/10.1016/j.mineng.2007.11.010.

Caraballo, M.A., Rimstidt, J.D., Macías, F., Nieto, J.M., Hochella, M.F., 2013. Metastability, nanocrystallinity and pseudo-solid solution effects on the understanding of schwertmannite solubility. Chem. Geol. 360–361, 22–31. https://doi.org/10.1016/j.chemgeo.2013.09.023.

Carbone, C., Dinelli, E., Marescotti, P., Gasparotto, G., Lucchetti, G., 2013. The role of AMD secondary minerals in controlling environmental pollution: Indications from bulk leaching tests. J. Geochem. Explor. 132, 188–200. https://doi.org/10.1016/j.gexplo.2013.07.001.

Consani, S., Ianni, M.C., Dinelli, E., Capello, M., Cutroneo, L., Carbone, C., 2019. Assessment of metal distribution in different Fe precipitates related to Acid Mine Drainage through two sequential extraction procedures. J. Geochem. Explor. 196, 247–258. https://doi.org/10.1016/j.gexplo.2018.10.010.

Córdoba, E.M., Muñoz, J.A., Blázquez, M.L., González, F., Ballester, A., 2008a. Leaching of chalcopyrite with ferric ion. Part I: general aspects. Hydrometallurgy 93, 81–87. https://doi.org/10.1016/j.hydromet.2008.04.015.

Córdoba, E.M., Muñoz, J.A., Blázquez, M.L., González, F., Ballester, A., 2008b. Leaching of chalcopyrite with ferric ion. Part II: effect of redox potential. Hydrometallurgy 93, 88–96. https://doi.org/10.1016/j.hydromet.2008.04.016.

Cuvier, A., Leleyter, L., Probst, A., Probst, J.-L., Prunier, J., Pourcelot, L., Le Roux, G., Lemoine, M., Reinert, M., Baraud, F., 2021. Why comparison between different chemical extraction procedures is necessary to better assess the metals availability in sediments. J. Geochem. Explor. 225, 106762 https://doi.org/10.1016/j.gexplo.2021.106762.

Descostes, M., Vitorge, P., Beaucaire, C., 2004. Pyrite dissolution in acidic media. Geochim. Cosmochim. Acta 68, 4559–4569. https://doi.org/10.1016/j.gca.2004.04.012.

Dold, B., 2003a. Speciation of the most soluble phases in a sequential extraction procedure adapted for geochemical studies of copper sulfide mine waste. J. Geochem. Explor. 80, 55–68. https://doi.org/10.1016/S0375-6742(03)00182-1.

Dold, B., 2003b. Dissolution kinetics of schwertmannite and ferrihydrite in oxidized mine samples and their detection by differential X-ray diffraction (DXRD). Appl. Geochem. 18, 1531–1540. https://doi.org/10.1016/S0883-2927(03)00015-5.

Dold, B., 2008. Sustainability in metal mining: from exploration, over processing to mine waste management. Rev. Environ. Sci. Biotechnol. 7, 275. https://doi.org/10.1007/s11157-008-9142-y.

Dold, B., 2010. Basic concepts in environmental geochemistry of sulfidic mine-waste management. In: Kumar, S. (Ed.), Waste Management, pp. 173–198 http://www.intechopen.com/books/waste-management/basic-concepts-inenvironmental-geochemistry-of-sulfidic-mine-waste-management.

Dold, B., 2017. Acid rock drainage prediction: a critical review. J. Geochem. Explor. 172, 120–132. https://doi.org/10.1016/j.gexplo.2016.09.014.

Dold, B., Fontboté, L., 2001. Element cycling and secondary mineralogy in porphyry copper tailings as a function of climate, primary mineralogy, and mineral processing. J. Geochem. Explor. 74, 3–55. https://doi.org/10.1016/S0375-6742(01)00174-1.

Dold, B., Fontboté, L., 2002. A mineralogical and geochemical study of element mobility in sulfide mine tailings of Fe oxide Cu–Au deposits from the Punta del Cobre belt, northern Chile. Chem. Geol. 189, 135–163. https://doi.org/10.1016/S0009-2541(02)00044-X.

Dold, B., Weibel, L., 2013. Biogeometallurgical pre-mining characterization of ore deposits: an approach to increase sustainability in the mining process. Environ. Sci. Pollut. Res. 20, 7777–7786. https://doi.org/10.1007/s11356-013-1681-2.

Elghali, A., Benzaazoua, M., Bouzahzah, H., Bussière, B., Villarraga-Gómez, H., 2018. Determination of the available acid-generating potential of waste rock, part I: mineralogical approach. Appl. Geochem. 99, 31–41. https://doi.org/10.1016/j.apgeochem.2018.10.021.

Elsherief, A.E., Saba, A.E., Afifi, S.E., 1995. Anodic leaching of chalcocite with periodic cathodic reduction. Miner. Eng. 8, 967–978. https://doi.org/10.1016/0892-6875(95)00060-4.

Filipek, L.H., Theobald Jr., P.K., 1981. Sequential extraction techniques applied to a porphyry copper deposit in the basin and range province. J. Geochem. Explor. 14, 155–174. https://doi.org/10.1016/0375-6742(81)90110-2.

Fisher, W.W., 1994. Comparison of chalcocite dissolution in the sulfate, perchlorate, nitrate, chloride, ammonia, and cyanide systems. Miner. Eng. 7, 99–103. https://doi.org/10.1016/0892-6875(94)90150-3.

Fisher, W.W., Flores, F.A., Henderson, J.A., 1992. Comparison of chalcocite dissolution in the oxygenated, aqueous sulfate and chloride systems. Miner. Eng. 5, 817–834. https://doi.org/10.1016/0892-6875(92)90248-8.

Fox, N., Parbhakar-Fox, A., Moltzen, J., Feig, S., Goemann, K., Huntington, J., 2017. Applications of hyperspectral mineralogy for geoenvironmental characterisation. Miner. Eng. 107, 63–77. https://doi.org/10.1016/j.mineng.2016.11.008.

Gray, C.A., Van Rythoven, A.D., 2020. A comparative study of porphyry-type copper deposit mineralogies by portable X-ray fluorescence and optical petrography. Minerals 10, 431. https://doi.org/10.3390/min10050431.

Guanira, K., Valente, T.M., Ríos, C.A., Castellanos, O.M., Salazar, L., Lattanzi, D., Jaime, P., 2020. Methodological approach for mineralogical characterization of tailings from a Cu(Au,Ag) skarn type deposit using QEMSCAN (Quantitative Evaluation of Minerals by Scanning Electron Microscopy). J. Geochem. Explor. 209, 106439 https://doi.org/10.1016/j.gexplo.2019.106439.

Guseva, O., Opitz, A.K.B., Broadhurst, J.L., Harrison, S.T.L., Becker, M., 2021. Characterisation and prediction of acid rock drainage potential in waste rock: value of integrating quantitative mineralogical and textural measurements. Miner. Eng. 163, 106750 https://doi.org/10.1016/j.mineng.2020.106750.

Hall, G.E.M., Vaive, J.E., Beer, R., Hoashi, M., 1996. Selective leaches revisited, with emphasis on the amorphous Fe oxyhydroxide phase extraction. J. Geochem. Explor. 56, 59–78. https://doi.org/10.1016/0375-6742(95)00050-X.

Hewitt, D.M., Breuer, P.L., Jeffrey, M.I., Naim, F., 2009. Mechanisms of sulfide ion oxidation during cyanidation. Part II: surface catalysis by pyrite. Miner. Eng. 22, 1166–1172. https://doi.org/10.1016/j.mineng.2009.06.002.

Jacques, S., Greet, C.J., Bastin, D., 2016. Oxidative weathering of a copper sulphide ore and its influence on pulp chemistry and flotation. Miner. Eng. 99, 52–59.

Jennings, S.R., Dollhopf, D.J., Inskeep, W.P., 2000. Acid production from sulfide minerals using hydrogen peroxide weathering. Appl. Geochem. 15, 235–243. https://doi.org/10.1016/S0883-2927(99)00041-4.

Khorasanipour, M., 2015. Environmental mineralogy of Cu-porphyry mine tailings, a case study of semi-arid climate conditions, Sarcheshmeh mine, SE Iran. J. Geochem. Explor. 153, 40–52. https://doi.org/10.1016/j.gexplo.2015.03.001.

Kitson, R.E., 1950. Simultaneous spectrophotometric determination of cobalt, copper, and iron. Anal. Chem. 22, 664–667. https://doi.org/10.1021/ac60041a012.

Lichtner, P.C., Biino, G.G., 1992. A first principles approach to supergene enrichment of a porphyry copper protore: I. Cu-Fe-S subsystem. Geochim. Cosmochim. Acta 56, 3987–4013. https://doi.org/10.1016/0016-7037(92)90012-8.

Liu, Z., Yin, Z., Hu, H., Chen, Q., 2012. Leaching kinetics of low-grade copper ore containing calcium-magnesium carbonate in ammonia-ammonium sulfate solution with persulfate. Trans. Nonferrous Met. Soc. China 22, 2822–2830. https://doi.org/10.1016/S1003-6326(11)61538-0.

Lundström, M., Liipo, J., Aromaa, J., 2012. Dissolution of copper and iron from sulfide concentrates in cupric chloride solution. Int. J. Miner. Process. 102–103, 13–18. https://doi.org/10.1016/j.minpro.2011.11.005.

Miki, H., Nicol, M., Velásquez-Yévenes, L., 2011. The kinetics of dissolution of synthetic covellite, chalcocite and digenite in dilute chloride solutions at ambient temperatures. Hydrometallurgy 105, 321–327. https://doi.org/10.1016/j.hydromet.2010.11.004.

Nicol, M., Miki, H., Velásquez-Yévenes, L., 2010. The dissolution of chalcopyrite in chloride solutions: part 3. Mechanisms. Hydrometallurgy 103, 86–95. https://doi.org/10.1016/j.hydromet.2010.03.003.

Oraby, E.A., Eksteen, J.J., 2014. The selective leaching of copper from a gold–copper concentrate in glycine solutions. Hydrometallurgy 150, 14–19. https://doi.org/10.1016/j.hydromet.2014.09.005.

Oraby, E.A., Eksteen, J.J., Tanda, B.C., 2017. Gold and copper leaching from gold-copper ores and concentrates using a synergistic lixiviant mixture of glycine and cyanide. Hydrometallurgy 169, 339–345. https://doi.org/10.1016/j.hydromet.2017.02.019.

Ossandón, G., Fréraut, R., Gustafson, L.B., Lindsay, D.D., Zentilli, M., 2001. Geology of the Chuquicamata mine: a progress report. Econ. Geol. 96, 249–270. https://doi.org/10.2113/gsecongeo.96.2.249.

Petre, C.F., Larachi, F., 2006. Capillary electrophoretic separation of inorganic sulfur-sulfide, polysulfides, and sulfur-oxygen species. J. Sep. Sci. 29, 144–152. https://doi.org/10.1002/jssc.200500265.

Petre, C.F., Azizi, A., Olsen, C., Baçaoui, A., Larachi, F., 2008. Capillary electrophoretic analysis of sulfur and cyanicides speciation during cyanidation of gold complex sulfidic ores. J. Sep. Sci. 31, 3902–3910. https://doi.org/10.1002/jssc.200800416.

Piché, S., Larachi, F., 2007. Hydrosulfide oxidation pathways in oxic solutions containing iron(III) chelates. Environ. Sci. Technol. 41, 1206–1211. https://doi.org/10.1021/es061752h.

Pinget, M.-C., 2016. Supergene Enrichment and Exotic Mineralization at Chuquicamata, Chile. Ph.D. thesis. Section of Earth and Evironmental Sciences, University of Geneva. https://doi.org/10.13097/archive-ouverte/unige:91513.

Pooler, R., Dold, B., 2017. Optimization and quality control of automated quantitative mineralogy analysis for acid rock drainage prediction. Minerals 7, 12. https://doi.org/10.3390/min7010012.

Preece, R.K., Williams, M.J., Gilligan, J.M., 2018. Development of partial extraction methods to estimate abundance of copper-iron sulphide minerals in the Escondida Norte porphyry copper deposit, Chile. Geochem.-Explor. Environ. A 18, 13–30. https://doi.org/10.1144/geochem2017-002.

Roebbert, Y., Rabe, K., Lazarov, M., Schuth, S., Schippers, A., Dold, B., Weyer, S., 2018. Fractionation of Fe and Cu isotopes in acid mine tailings: modification and application of a sequential extraction method. Chem. Geol. 493, 67–79. https://doi.org/10.1016/j.chemgeo.2018.05.026.

Ruiz-Sánchez, A., Lapidus, G.T., 2017. Study of chalcopyrite leaching from a copper concentrate with hydrogen peroxide in aqueous ethylene glycol media. Hydrometallurgy 169, 192–200. https://doi.org/10.1016/j.hydromet.2017.01.014.

Sahuquillo, A., Rigol, A., Rauret, G., 2003. Overview of the use of leaching/extraction tests for risk assessment of trace metals in contaminated soils and sediments. TrAC Trends Anal. Chem. 22, 152–159. https://doi.org/10.1016/S0165-9936(03)00303-0.

Sarveswara Rao, K., Ray, H.S., 1998. A new look at characterisation and oxidative ammonia leaching behaviour of multimetal sulphides. Miner. Eng. 11, 1011–1024. https://doi.org/10.1016/S0892-6875(98)00089-2.

Scheffel, R.E., Guzman, A., Dreier, J.E., 2016. Development metallurgy guidelines for copper heap leach. Miner. Metall. Proc. 33, 187–199. https://doi.org/10.19150/mmp.6840.

Senanayake, G., 2009. A review of chloride assisted copper sulfide leaching by oxygenated sulfuric acid and mechanistic considerations. Hydrometallurgy 98, 21–32. https://doi.org/10.1016/j.hydromet.2009.02.010.

Sokić, M.D., Marković, B., Živković, D., 2009. Kinetics of chalcopyrite leaching by sodium nitrate in sulphuric acid. Hydrometallurgy 95, 273–279. https://doi.org/10.1016/j.hydromet.2008.06.012.

Sondag, F., 1981. Selective extraction procedures applied to geochemical prospecting in an area contaminated by old mine workings. In: Rose, A.W., Gundlach, H. (Eds.), Developments in Economic Geology, Geochemical Exploration, 1980. Elsevier, pp. 645–652. https://doi.org/10.1016/B978-0-444-42012-1.50047-7.

Sutherland, R.A., 2010. BCR®-701: a review of 10-years of sequential extraction analyses. Anal. Chim. Acta 680, 10–20. https://doi.org/10.1016/j.aca.2010.09.016.

Teel, A.L., Finn, D.D., Schmidt, J.T., Cutler, L.M., Watts, R.J., 2007. Rates of trace mineral-catalyzed decomposition of hydrogen peroxide. J. Environ. Eng. 133, 853–858. https://doi.org/10.1061/(ASCE)0733-9372(2007)133:8(853).

Torres, E., Auleda, M., 2013. A sequential extraction procedure for sediments affected by acid mine drainage. J. Geochem. Explor. 128, 35–41. https://doi.org/10.1016/j.gexplo.2013.01.012.

Velásquez, G., Estay, H., Vela, I., Salvi, S., Pablo, M., 2020. Metal-selective processing from the Los Sulfatos porphyry-type deposit in Chile: Co, Au, and Re recovery workflows based on advanced geochemical characterization. Minerals 10, 531. https://doi.org/10.3390/min10060531.

Velásquez-Yévenes, L., Nicol, M., Miki, H., 2010. The dissolution of chalcopyrite in chloride solutions: part 1. The effect of solution potential. Hydrometallurgy 103, 108–113. https://doi.org/10.1016/j.hydromet.2010.03.001.

Vračar, R.Ž., Vučković, N., Kamberović, Ž., 2003. Leaching of copper(I) sulphide by sulphuric acid solution with addition of sodium nitrate. Hydrometallurgy 70, 143–151. https://doi.org/10.1016/S0304-386X(03)00075-6.

Wang, H., Wen, S., Han, G., Feng, Q., 2021. Modification of malachite surfaces with lead ions and its contribution to the sulfidization flotation. Appl. Surf. Sci. 550, 149350 https://doi.org/10.1016/j.apsusc.2021.149350.

Whitney, D.L., Evans, B.W., 2010. Abbreviations for names of rock-forming minerals. Am. Mineral. 95, 185–187. https://doi.org/10.2138/am.2010.3371.

Xian, Y.J., Wen, S.M., Deng, J.S., Liu, J., Nie, Q., 2012. Leaching chalcopyrite with sodium chlorate in hydrochloric acid solution. Can. Metall. Q. 51, 133–140. https://doi.org/10.1179/1879139512Y.0000000001.

Zhang, Q., Wen, S., Feng, Q., Liu, J., 2021a. Surface modification of azurite with lead ions and its effects on the adsorption of sulfide ions and xanthate species. Appl. Surf. Sci. 543, 148795 https://doi.org/10.1016/j.apsusc.2020.148795.

Zhang, Q., Wen, S., Feng, Q., Liu, Y., 2021b. Activation mechanism of lead ions in the flotation of sulfidized azurite with xanthate as collector. Miner. Eng. 163, 106809 https://doi.org/10.1016/j.mineng.2021.106809.